IEEE Access
Multidisciplinary | Rapid Review | Open Access Journal

Received September 2, 2019, accepted September 8, 2019, date of publication October 15, 2019, date of current version October 28, 2019.

Digital Object Identifier 10.1109/ACCESS.2019.2947023

A Novel Second Order Repetitive Control That Facilitates Stability Analysis and Its Application to Magnetically Suspended Rotors

PEILING CUI[1], (Member, IEEE), ZHIYUAN LIU[1], GUOXI ZHANG[1], HAN XU[1], AND RICHARD W. LONGMAN[2]

[1]School of Instrumentation and Optoelectronic Engineering, Beihang University, Beijing 100191, China
[2]Department of Mechanical Engineering, Columbia University, New York, NY 10027, USA

Corresponding author: Peiling Cui (cuiplhh@126.com)

This work was supported in part by the National Natural Science Foundation of China under Grant 61673044, and in part by the National Key Research and Development Plan under Grant 2016YFB0500804.

ABSTRACT Repetitive control is an effective method to eliminate the effects of a periodic disturbance on a control system. In some applications the period is not known with sufficient accuracy, or the period may fluctuate sufficiently to seriously compromise performance. Second order repetitive control has been developed in response to this issue. Existing methods of analyzing stability for such systems are either very difficult to use, or excessively conservative sufficient conditions. A novel second order repetitive control is proposed here which achieves the behavior of second order but uses data from only one period in the past. This better meets the requirements for real time storage, but more importantly, it allows us to develop a stability criterion that is much less conservative. The experimental results demonstrate that the suppression effect can achieve a high level under frequency fluctuation with the proposed control method.

INDEX TERMS Frequency fluctuation, harmonic suppression, magnetically suspended rotor, second order repetitive control, periodic disturbance cancellation.

I. INTRODUCTION

A novel form of second order repetitive control (RC) is proposed in this paper, which can greatly facilitate the stability analysis. The motivation of the study originates from the urgent requirements of micro-vibration spacecraft. Spacecraft often suffer from vibrations produced by the rotating wheels used as attitude control actuators, i.e., reaction wheels or control moment gyros [1]. This degrades the performance of fine pointing equipment on board. Passive vibration isolation methods have limited performance, hence active vibration cancellation strategies are considered [2]. Laser communications between spacecrafts or with ground offer a different option of canceling the influence of spacecraft jitter by control methods applied to pan and tilt of the outgoing mirror [3] that cancels vibrations in the beam. The hardware demonstration of the proposed second order repetitive control approach, considers magnetically suspended rotor (MSR) performance, which can have disturbances of rotor mass imbalance and sensor runout. The objective is to reduce the vibrations at their source in the spacecraft, instead of at the sensor location of fine pointing equipment by vibration isolation.

The mass imbalance of the rotor and the sensor runout are two kinds of vibration sources. Mass imbalance of the rotor will result in synchronous current stiffness force and synchronous displacement stiffness force. Sensor runout will result in synchronous and multi-frequency (collectively called harmonic) current stiffness force. Then, the vibration force includes the harmonic current stiffness force and synchronous displacement stiffness force. This paper aims to reduce the vibrations by suppressing the harmonic current stiffness force, and the corresponding approach is to suppress the periodic components in harmonic current.

Sliding-mode control has been used to suppress periodic uncertainties [4], [5] for good transient response and robustness, but the chattering phenomenon brought by actuator limitations or time discretization will reduce the control accuracy and the system performance. A resonant control strategy with phase compensation [6] can suppress the periodic disturbance

The associate editor coordinating the review of this manuscript and approving it for publication was Jianyong Yao.

components, with effective experimental results achieved in a magnetic bearing system. A nonlinear adaptive control using Fourier series approximation [7] provides an ingenious transformation from periodic disturbance to a series of trigonometric functions with unknown constant gains, and a successful verification has been provided for hydraulic servo systems. Zheng *et al.* [8] apply the phase-shift notch filters to harmonic disturbance elimination, and the stability can be ensured by the phase shift angle. However, these methods containing trigonometric functions or Fourier series may raise the computation burden.

Repetitive control is one main approach among several controllers that can be used for harmonic suppression [3], [9], [10]. RC assumes that the disturbance period is known, which is reasonable because the speed of the rotor is under control. Algorithms initially can aim to correct the frequencies of the given period, fundamental, and all harmonics up to Nyquist frequency. Using the equivalent of a discrete time integral control at each frequency eliminates periodic disturbance effects at these frequencies. At each time step, the current command to a control system is adjusted based on the error seen in the previous period. A difficulty is that performance of conventional RC (CRC) can be very sensitive to accurate knowledge of the period, and to any fluctuation of that period with time [11]. In CRC one can only adjust the overall gain to influence the sensitivity. Trying to converge fast is somewhat beneficial, but this decreases the robustness to this period error.

Various approaches have been developed to better address the sensitivity to the uncertainty. These include higher order RC (HORC) [12]–[20], alternative of using ILC designed for multiple unrelated periods in the disturbance, and making two periods be the same [21]. Minor but non-negligible clock error drift, jitter, measurement noise and other factors produce period variations, and [15], [17] suggest a need for accuracy of $\pm 0.1\%$, and while running experiments in [3] the accuracy limitation of Hall sensors was insufficient to be used for CRC. The MSR system studied here requires the method to reduce sensitivity.

Repetitive control systems require a compensator to cancel much of the phase change going through the plant in order to be stable. Due to excessive uncertainties and varying disturbances, an accurate model is not available. Phase errors in the plant compensation add to the phase errors resulting from an inaccurate disturbance period, making this insensitivity still more important.

At each time step CRC looks at the error and command one period back (adjusted for the time delay through the system), and modifies the current input, aiming to converge to zero error. HORC looks back more than one period. One might consider doing this with positive weights for each period, and then one is making a weighted average. This could be beneficial by reducing the effects of measurement noise, but the same effect can be gained much more simply by reducing the repetitive control gain so that less importance is placed on the latest measurement. In order to address the insensitivity objective, one must use some negative weights on errors more than one period back. References [13] and [14] show the range of possible behaviors viewed from root locus analysis and from frequency response analysis. Reference [20] presents a straightforward design procedure to optimize performance (see also [18]). Others pick weights based on an optimization criterion [12], [15], [16]. Underlying these methods are just three principles. (1) In CRC, the sensitivity transfer function from output disturbance to error has a cusp going to zero at the addressed frequency. If the poles on the unit circle of the CRC are repeated once, making second order RC (SORC), then the cusp is replaced by a valley with a zero derivative at the bottom. Then the walls of the cusp as frequency deviates from nominal, become the walls of the valley with more separation, decreasing the sensitivity to frequency or period errors. Third order RC makes the poles for each frequency on the unit circle appear three times. (2) Since one is putting more poles on the unit circle, one can decide to separate them a small amount, making the sensitivity transfer function become zero at two or three values at the bottom of the valley. Reference [20] presents a design approach for making these adjustments. (3) One can also move the new roots introduced slightly inside the unit circle.

SORC is chosen here. Higher order RC is conditionally stable as one turns up the gain, being unstable until a specific gain is reached when the locus comes into the unit circle after having departed with an outward component. This paper presents a novel form of SORC. In place of the usual SORC that uses two periodic signal generators in series, a method is developed here using two periodic signal generators in parallel. This allows one to implement SORC using only data from one period back, and yet have the same performance as standard SORC that takes data from two periods back. There are of course, benefits of reducing command and error storage requirements, but the main benefit is that it allows us to create a sufficient stability criterion that is vastly simpler and much less conservative than the existing methods of analyzing HORC.

The rest of this paper is organized as follows. The problem statement is given in Section II. Section III presents the new second order repetitive control. Experimental results are given in Section IV. Section V concludes this paper. The notation used in this paper is standard. For notational simplicity, the frequency response function of a discrete-time $H(z)$ is denoted by $H(\omega)$ instead of $H(e^{j\omega T_s})$.

II. PROBLEM STATEMENT

A. THE BLOCK DIAGRAM OF THE "STANDARD" SORC

The ''standard'' SORC as in [12]–[20] is depicted in Fig.1.

The transfer function from $i(z)$ to $i_{rc}(z)$ is given as follows:

$$G_{src}(z) = k_{rc}\frac{W(z)}{1 - W(z)} \tag{1}$$

where k_{rc} is the control gain; $i(z)$ in application considered here is the harmonic current of the rotor which the SORC is to suppress; $i_{rc}(z)$ is the output of $i(z)$ after the target controller;

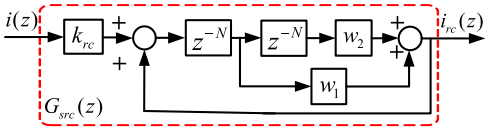

FIGURE 1. Schematic of the "standard" SORC.

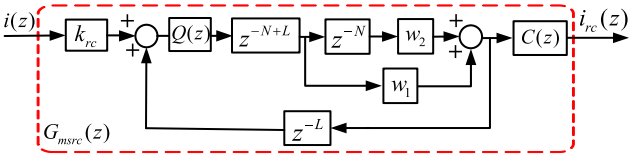

FIGURE 2. The block diagram of the modified SORC.

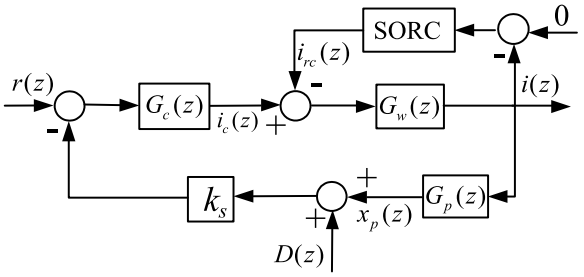

FIGURE 3. Block diagram of SORC for the MSR system.

N is the number of time steps of length T_s in one disturbance period $T_0 = NT_s$ (N is an integer, otherwise interpolation is used); $W(z) = w_1 z^{-N} + w_2 z^{-2N}$, w_1 and w_2 are the proper signal weights to obtain period variation robustness and improve the performance.

For CRC, $w_2 = 0$ which results in $W(z) = z^{-N}$, and just retrieves error one period back. And the denominator $1-W(z)$ of $G_{src}(z)$ evaluated at frequencies by setting $z = e^{j\omega T_s}$ is zero at the fundamental, and all harmonics. For ''standard'' SORC, $W(z) = w_1 z^{-N} + w_2 z^{-2N}$ retrieving error from one period and two periods back. The denominator being zero at the frequencies of period T_0 ensures convergence to zero at targeted frequencies, provided $w_1 + w_2 = 1$ [15]. Because of the use of multiple delay lines, the control signal of the ''standard'' SORC can be computed as a weighted sum of the signals of one, and two periods back.

From [13], $|w_2| < 1$ ensures poles of the $G_{src}(z)$ are inside the unit circle, with the exception of the original N poles on the unit circle. Thus, the range of possible choices of the parameter w_2 is restricted to: $-1 < w_2 < 0$, or $0 < w_2 < 1$. The case of $w_2 = 0$ is eliminated since it reduces SORC to CRC.

B. PLUG-IN MODIFIED SORC OF THE MSR SYSTEM

Fig. 1 portrays the ''standard'' SORC, but high-frequency components and system uncertainty may lead the system to instability due to the poles on the unit circle generated by $G_{src}(z)$ up to Nyquist frequency. Therefore, in order to provide high-enough robustness margins, low-pass filters are usually introduced to improve the robustness of the whole systems in real applications by not aiming to cancel high frequency periodic errors where the model uncertainty is large.

Fig. 2 depicts the block diagram of the modified SORC within the dashed block, and the transfer function is:

$$G_{msrc}(z) = k_{rc}\frac{W(z)Q(z)}{1-W(z)Q(z)}L(z)C(z) \tag{2}$$

wherein $Q(z)$ is the zero-phase low-pass filter used for stability robustness to high frequency model error; $C(z)L(z)$ is a compensator, ideally equal to the inverse of the system frequency response. $C(z)$is a phase compensator to reduce the large phase change of the MSR plant whose model is uncertain; $L(z) = z^L$ is chosen here to be a linear phase lead compensator with L being the lead-step of $L(z)$ [22]–[24] and it is realized in the feedback branch.

Fig. 3 shows the overall structure of the MSR system studied in [11]. $G_c(z)$ is a pre-stabilizing feedback controller, which implies a pre-stable baseline feedback loop and responds to the reference displacement $r(z)$. The stable rotation of rotor is the precondition for suppressing the harmonic current. SORC is used to suppress the harmonic components in current $i(z)$. $G_w(z)$ and $G_p(z)$ are transfer functions of the power amplifier and the rotor, respectively. k_s is the sensor gain. The periodic disturbance $D(z)$ is the equivalent periodic disturbance of the sensor runout and the mass imbalance of the rotor.

The transfer function of the plant as seen by the SORC is

$$F(z) = \frac{G_w(z)}{1 + k_s G_p(z) G_c(z) G_w(z)} \tag{3}$$

The transfer function from $D(z)$ to $i(z)$ is

$$G(z) = G_0(z)\frac{1 - W(z)Q(z)}{1 - W(z)Q(z)X(z)} \tag{4}$$

with $G_0(z) = -k_s G_c(z)F(z)$ giving the transfer function of Fig. 3 from $D(z)$ to $i(z)$ without the SORC, and $X(z) = 1 + k_{rc}C(z)L(z)F(z)$. For future use, write the frequency transfer functions $C(z)$, $F(z)$ and $L(z)$ represented in terms of magnitude and phase as $C(\omega) = A_c(\omega)e^{j\theta_c(\omega)}$, $F(\omega) = A_f(\omega)e^{j\theta_f(\omega)}$, and $L(\omega) = e^{j\omega LT_s}$, respectively. Then define the magnitude and phase of the product $C(z)L(z)F(z)$ as $M(\omega) = A_c(\omega)A_f(\omega)$ and $\theta(\omega) = \theta_c(\omega) + \theta_f(\omega) + \omega LT_s$.

C. PERSPECTIVE ON STABILITY CONDITIONS

This section aims for a general understanding of possible RC stability conditions. Given that $G_0(z)$ is asymptotically stable, and for simplicity consider that $Q(z) = 1$, then the characteristic equation of interest in (4) is $1 - W(z)X(z) = 0$.

Consider CRC: For CRC, $W(z) = z^{-N}$. Directly finding the roots with a root finding algorithm is impractical because N can be very large, e.g., sampling at 500Hz with a 2s desired period makes $N = 1000$. Direct application of Nyquist stability criterion is also impractical because there are N roots on the unit circle, i.e., the discrete time Nyquist contour should go around each. Reformulation eliminates this

problem [25], [26]. The result is a condition (i) asking that $z^{-N}X(z)$ does not encircle $+1$ as ω goes around the unit circle. This is difficult to plot because as ω goes from zero to Nyquist, the phase of z goes from zero to π, and the phase of z^{-N} goes to $-N\pi$, spinning many times; (ii) asking that $\left|z^{-N}X(z)\right| < 1$ for all ω, creating a sufficient condition, which can be simplified producing the following condition; (iii) asking that $|X(z)| < 1$. Because $X(z)$ does not depend on N, condition (iii) is a particularly simple criterion to use. Although this is only a sufficient condition, [26] and [27] show that failing to satisfy it and still having stability can only happen for very small N because of the spin.

Consider SORC: For SORC, $W(z) = w_1z^{-N} + w_2z^{-2N}$. Condition (i) applies to $W(z)X(z)$ as a sufficient condition [17]. The condition (ii) becomes $|(w_1z^{-N} + w_2z^{-2N})X(z)| < 1$. Again it simplifies to (iii) giving $|(w_1 + w_2z^{-N})X(z)| < 1$. Further, a novel still more restrictive sufficient condition (iv) can be generated, requiring $|X(z)| < 1/\max\left|(w_1 + w_2z^{-N})\right|$, or equivalently $|X(z)| < 1/\max_{\omega}|W(z)|$ for all ω.

D. STABILITY CONDITION PROOFS FOR THE MODIFIED SORC

Theorem 1: The closed-loop system in Fig. 3 with modified SORC of Fig. 2 is asymptotically stable for $Q(z) = 1$ if:

1. The original closed loop transfer function $G_0(z)$, is asymptotically stable,

2.a. And either $\|W(z)X(z)\|_\infty < 1$, for all $z = e^{j\omega T_s}$, $0 \le \omega < \omega_m$, where ω_m is Nyquist frequency, $\|\|_\infty$ denotes the H_∞-norm of a stable transfer function.

2.b. Or $|X(z)| < 1/\|W(z)\|_\infty$ for all $z = e^{j\omega T_s}$, $0 \le \omega < \omega_m$. In this case: $\|W(z)\|_\infty = 1$ if $0 < w_2 < 1$; and $\|W(z)\|_\infty = 1 - 2w_2$ if $-1 < w_2 < 0$.

Proof: Item (2.b) of Theorem 1 is the sufficient condition (iv) above. It remains to show the bounds on $W(z)$:

$$\begin{aligned}|W(z)|_{z=e^{j\omega T_s}} &= \left|w_1e^{-j\omega T_0} + w_2e^{-j2\omega T_0}\right| \\ &= |w_1(\cos\omega T_0 - j\sin\omega T_0) \\ &\quad + w_2(\cos 2\omega T_0 - j\sin 2\omega T_0)| \\ &= \sqrt{\left|w_1^2 + w_2^2 + 2w_1w_2\cos\omega T_0\right|} \end{aligned} \quad (5)$$

When both w_1 and w_2 are between 0 and 1, this is less than or equal to $\sqrt{\left|w_1^2 + w_2^2 + 2w_1w_2\right|} = |w_1 + w_2| = 1$, and when ω equals zero it is equal to 1. Therefore $\|W(z)\|_\infty = 1$. When $1 < w_1 \le 2$ and $-1 < w_2 < 0$, it is less than or equal to $\sqrt{\left|w_1^2 + w_2^2 - 2w_1w_2\right|} = |w_1 - w_2| = 1 - 2w_2$, and the equality holds when ω is π. Therefore $\|W(z)\|_\infty = 1 - 2w_2$.

The proof is complete.

Based on Theorem 1, the following theorem explicitly provides the bounds of k_{rc} and $\theta(\omega)$ which can make the whole system stable:

Theorem 2: If the following conditions on k_{rc} and $\theta(\omega)$ are satisfied, then Item (2.b) of Theorem 1 is satisfied:

1. For $0 < w_2 < 1$

$$\begin{aligned} 0 < k_{rc} &< 2\min|\cos\theta(\omega)| \,/\, \max[M(\omega)]\,; \\ &\theta(\omega) \in (90°, 270°) \end{aligned} \quad (6)$$

2. For $-1 < w_2 < 0$

$$\begin{aligned} k_{rc} &\ge \max\left|\sqrt{(1-2w_2)^{-2} - \sin^2\theta(\omega)} + \cos\theta(\omega)\right| \\ &\quad / \min[M(\omega)] \\ k_{rc} &\le \min\left|\sqrt{(1-2w_2)^{-2} - \sin^2\theta(\omega)} - \cos\theta(\omega)\right| \\ &\quad / \max[M(\omega)] \\ \theta(\omega) &\in (180° - \arcsin[(1-2w_2)^{-1}], \\ &\quad 180° + \arcsin[(1-2w_2)^{-1}]) \end{aligned} \quad (7)$$

Proof:

1. For$0 < w_2 < 1$, and using $Q(z) = 1$ and $\omega \in (0, \omega_m)$, $|X(z)| \le 1$ can be written as

$$|1 + k_{rc}C(\omega)L(\omega)F(\omega)| = \left|1 + k_{rc}M(\omega)e^{j\theta(\omega)}\right| \le 1 \quad (8)$$

and

$$|1 + k_{rc}M(\omega)\,(\cos\theta(\omega) + j\sin\theta(\omega))| \le 1 \quad (9)$$

Squaring and cancelling the positive terms k_{rc} and $M(\omega)$ gives

$$k_{rc}M(\omega) \le -2\cos\theta(\omega) \quad (10)$$

$$k_{rc} \le -2\min(\cos\theta(\omega))/\max[M(\omega)] \quad (11)$$

Since $k_{rc} > 0$, angle $\theta(\omega) \in (90°, 270°)$.

2. Following an analogous sequence of steps for $-1 < w_2 < 0$, $|X(z)| \le (1-2w_2)^{-1}$ can be written as

$$\begin{aligned} |1 + k_{rc}C(\omega)L(\omega)F(\omega)| &= \left|1 + k_{rc}M(\omega)e^{j\theta(\omega)}\right| \\ &\le (1-2w_2)^{-1} \end{aligned} \quad (12)$$

Squaring the magnitude for each side produces

$$\begin{aligned} &[k_{rc}M(\omega)]^2 + 2k_{rc}M(\omega)\cos\theta(\omega) + 1 \\ &\quad \le (1-2w_2)^{-2} \end{aligned} \quad (13)$$

$$\begin{aligned} &[k_{rc}M(\omega) + \cos\theta(\omega)]^2 \\ &\quad \le (1-2w_2)^{-2} - \sin^2\theta(\omega) \end{aligned} \quad (14)$$

$$\begin{aligned} k_{rc} &\ge -\left[\sqrt{(1-2w_2)^{-2} - \sin^2\theta(\omega)} + \cos\theta(\omega)\right] \\ &\quad / \min[M(\omega)] \end{aligned} \quad (15)$$

$$\begin{aligned} k_{rc} &\le \left[\sqrt{(1-2w_2)^{-2} - \sin^2\theta(\omega)} - \cos\theta(\omega)\right] \\ &\quad / \max[M(\omega)] \end{aligned} \quad (16)$$

for $k_{rc} > 0$. And from the above two inequalities, we have

$$\cos\theta(\omega) < 0, \quad -1 < w_2 < 0 \quad (17)$$

$$\begin{aligned} \theta(\omega) &\in (180° - \arcsin[(1-2w_2)^{-1}], \\ &\quad 180° + \arcsin[(1-2w_2)^{-1}]) \end{aligned} \quad (18)$$

The proof is complete.

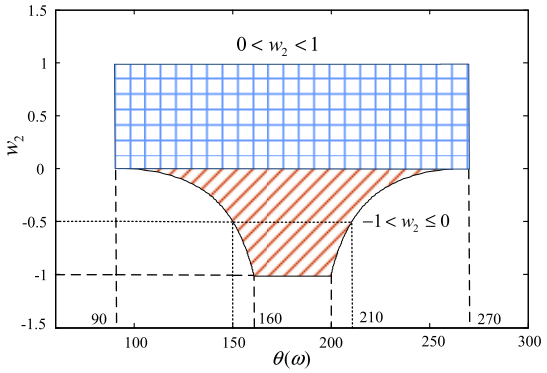

FIGURE 4. The relationship between w_2 and $\theta(\omega)$.

As for the robustness against to frequency fluctuations, as suggested in [12]–[19], one needs $w_2 < 0$ for the purpose of increasing robustness.

Fig. 4 depicts the relationship between $\theta(\omega)$ and w_2. The blue checkered region and red diagonal region, respectively, display the range of $\theta(\omega)$ with positive and negative w_2. It demonstrates that for positive w_2, the $\theta(\omega)$ has a wide range of phase stability, while for negative w_2 the tolerance on $\theta(\omega)$ becomes very restricted if stability needs to be guaranteed by using the condition of Theorem 1. For example, if $w_2 = -0.5$, then $\theta(\omega) \in (150°, 210°)$ is needed to guarantee stability. In the MSR application an accurate model is unavailable, and the phase error of the model after compensation can easily go beyond these limits, preventing one from designing a guaranteed stable system using the stability conditions discussed above. Of course, inaccurate knowledge of the period is also a phase error at the frequencies of interest.

Note that in the above discussion of the possible sufficient conditions, much difficulty is caused by the fact that in SORC there is a z^{-N} to deal with. In the next section, a novel SORC is developed, giving the same functionality, but with data only one period back. This novel control law allows us to develop a stability condition that bypasses these difficulties and is much more useful because it is not so conservative.

III. THE NOVEL SECOND ORDER REPETITIVE CONTROL DESIGN

A. BLOCK DIAGRAM OF A NOVEL SECOND ORDER REPETITIVE CONTROL

Fig. 5 depicts the block diagram of the novel second order RC schematic.

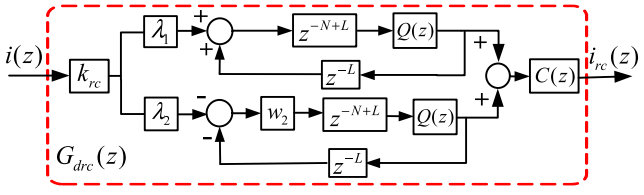

FIGURE 5. Schematic of the novel second order RC.

The transfer function from $i(z)$ to $i_{rc}(z)$ is

$$G_{drc}(z) = k_{rc}\left[\lambda_1 \frac{z^{-N}Q(z)}{1-z^{-N}Q(z)} - \lambda_2 \frac{w_2 z^{-N}Q(z)}{1+w_2 z^{-N}Q(z)}\right] L(z)C(z) \tag{19}$$

where $\lambda_1 = 1/(1+w_2)$, $\lambda_2 = w_2/(1+w_2)$, wherein $|w_2| < 1$, and $w_2 \neq 0$. The transfer function $G_{drc}(z)$ can be rewritten as:

$$G_{drc}(z) = \frac{k_{rc}}{1+w_2}\left[G_1(z) + G_2(z)\right] K_b(z) K_f(z) \tag{20a}$$

$$G_1(z) = \frac{z^{-N}Q(z)}{1-z^{-N}Q(z)},$$

$$G_2(z) = \frac{-w_2^2 z^{-N}Q(z)}{1+w_2 z^{-N}Q(z)} \tag{20b}$$

So, the internal model of (20) with$Q(z) = 1$, denoted as $\hat{G}_{drc}(z)$, matches that of SORC in (1):

$$\hat{G}_{drc}(z) = k_{rc}\left[\frac{(1-w_2)z^{-N} + w_2 z^{-2N}}{(1-z^{-N})(1+w_2 z^{-N})}\right] = G_{src}(z) \tag{21}$$

B. STABILITY CONDITION PROOFS FOR THE NOVEL SORC

The following theorem provides a sufficient stability criterion of the novel SORC in Fig. 5.

Theorem 3: The closed-loop MSR system in Fig. 3 with the novel SORC in Fig. 5 is asymptotically stable for all $-1 < w_2 < 1$, $w_2 \neq 0$, if:

1. The closed loop transfer function without SORC, $G_0(z)$, is asymptotically stable,
2. And

$$0 < k_{rc} < \frac{2(1+w_2)^2 \min|\cos\theta(\omega)|}{(1+w_2+2w_2^2)\max[M(\omega)]} \tag{22}$$

$$\theta(\omega) \in (90°, 270°) \tag{23}$$

Proof:

The transfer function from $D(z)$ to $i(z)$ in (3) can be rewritten as

$$G^*(z) = \frac{k_s G_c(z) F(z)}{1 - k_{rc} C(z) L(z) F(z) G^*_{drc}(z)} \tag{24}$$

$$G^*_{drc}(z) = \left[G_1(z) + G_2(z)\right]/(1+w_2) \tag{25}$$

Write $z = |z|\, e^{j\omega T_s}$ with $|z| = a$. Then

$$\begin{aligned} \mathrm{Re}\left[G_1(z)\right] &= \mathrm{Re}\left[Q(z)z^{-N}/(1-Q(z)z^{-N})\right] \\ &= \mathrm{Re}\left[a^N e^{j(N\omega T_s - \theta_q(\omega))}/A_q(\omega) - 1\right]^{-1} \end{aligned} \tag{26}$$

Let $b_1 = a^N/A_q(\omega)$ and $\theta_1 = L\omega T_s - \theta_q(\omega)$. With $|z| = a \geq 1$, we have $b_1 \geq a \geq 1$ due to $A_q(\omega) \leq 1$, then

$$\begin{aligned} \mathrm{Re}\left[G_1(z)\right] &= \mathrm{Re}(b_1 e^{j\theta_1} - 1)^{-1} \\ &= \frac{b_1\cos\theta_1 - 1}{b_1^2 + 1 - 2b_1\cos\theta_1} \end{aligned} \tag{27}$$

Examine the numerator, if it is non-negative, then

$$\mathrm{Re}\left[G_1(z)\right] = \frac{b_1\cos\theta_1 - 1}{b_1^2 + 1 - 2b_1\cos\theta_1} \geq 0 \tag{28}$$

and if it is negative

$$\frac{b_1^2+1-2b_1\cos\theta_1}{b_1\cos\theta_1-1}=\frac{b_1^2-1}{b_1\cos\theta_1-1}-2 \le \frac{a^2-1}{b_1\cos\theta_1-1}-2\le -2 \quad (29)$$

As a consequence

$$\mathrm{Re}\left[G_1(z)\right]\ge -(1/2);\quad \forall |z|=a\ge 1 \quad (30)$$

Now perform the analogous computations for $G_2(z)$ with $b_2=a^N/A_q(\omega)$ and $\theta_2=L\omega T_s-\theta_q(\omega)$. If $|z|=a\ge 1$, we have $b_2\ge a\ge 1$.

$$\mathrm{Re}\left[G_2(z)\right]=\mathrm{Re}\left[-w_2^2\frac{(b_2\cos\theta_2+w_2)-j(b_2\sin\theta_2)}{(b_2\cos\theta_2+w_2)^2+(b_2\sin\theta_2)^2}\right] =\frac{-w_2^2(b_2\cos\theta_2+w_2)}{(b_2\cos\theta_2+w_2)^2+(b_2\sin\theta_2)^2} \quad (31)$$

If $-(b_2\cos\theta_2+w_2)\ge 0$ one obtains

$$\mathrm{Re}\left[G_2(z)\right]=\frac{-w_2^2(b_2\cos\theta_2+w_2)}{(b_2\cos\theta_2+w_2)^2+(b_2\sin\theta_2)^2}\ge 0 \quad (32)$$

and if $-(b_2\cos\theta_2+w_2)<0$, for $|w_2|<1$, $\forall|z|=a\ge 1$ one obtains

$$\begin{aligned}&\frac{(b_2\cos\theta_2+w_2)^2+(b_2\sin\theta_2)^2}{-w_2^2(b_2\cos\theta_2+w_2)}\\ &=\frac{b_2^2+w_2^2+2b_2w_2\cos\theta_2}{-w_2^2(b_2\cos\theta_2+w_2)}\\ &\le\frac{b_2^2-w_2^2}{-w_2^2(b_2+w_2)}-\frac{2}{w_2}\le\frac{a-w_2}{-w_2^2}-\frac{2}{w_2}\\ &\le-\frac{1+w_2}{w_2^2}\end{aligned} \quad (33)$$

As a consequence

$$\mathrm{Re}\left[G_2(z)\right]\ge -w_2^2/(1+w_2);\quad \forall |z|=a\ge 1 \quad (34)$$

Therefore, $\forall|w_2|<1$, $w_2\ne 0$

$$\min_{|z|\ge 1}\mathrm{Re}\left[k_{rc}G_{drc}^*(z)\right]\ge\min_{|z|\ge 1}\left(k_{rc}\frac{1}{1+w_2}\left(-\frac{1}{2}-\frac{w_2^2}{1+w_2}\right)\right) \quad (35)$$

Apply the conditions (22) and (23) to (35), then

$$\min_{|z|\ge 1}\mathrm{Re}\left[k_{rc}G_{drc}^*(z)\right]>-\frac{1}{2}\cdot\frac{-2\cos\theta(\omega)}{\max\left[M(\omega)\right]}=\frac{\cos\theta(\omega)}{\max\left[M(\omega)\right]} \quad (36)$$

Set $z=e^{j\omega T_s}$, then

$$\begin{aligned}&1-k_{rc}C(\omega)L(\omega)F(\omega)G_{drc}^*(z)\\ &=1-M(\omega)e^{j\theta(\omega)}\left\{\mathrm{Re}\left[k_{rc}G_{drc}^*(z)\right]+j\,\mathrm{Im}\left[k_{rc}G_{drc}^*(z)\right]\right\}\\ &=1-M(\omega)\left\{\cos\theta(\omega)\mathrm{Re}\left[k_{rc}G_{drc}^*(z)\right]\right.\\ &\quad-\sin\theta(\omega)\mathrm{Im}\left[k_{rc}G_{drc}^*(z)\right]\}\\ &\quad-jM(\omega)\left\{\sin\theta(\omega)\mathrm{Re}\left[k_{rc}G_{drc}^*(z)\right]\right.\\ &\quad+\cos\theta(\omega)\mathrm{Im}\left[k_{rc}G_{drc}^*(z)\right]\}\end{aligned} \quad (37)$$

For the imaginary part to be zero

$$\mathrm{Im}\left[k_{rc}G_{drc}^*(\omega)\right]=-(\sin\theta(\omega)/\cos\theta(\omega))\mathrm{Re}\left[k_{rc}G_{drc}^*(\omega)\right] \quad (38)$$

Due to $\cos\theta(\omega)<0$ and $\forall|z|\ge 1$, we obtain

$$\begin{aligned}&1-k_{rc}C(z)L(z)F(z)G_{drc}^*(z)\\ &=1-M(\omega)\left\{\cos\theta(\omega)+\sin^2\theta(\omega)\Big/\cos\theta(\omega)\right\}\\ &\quad\times\mathrm{Re}\left[k_{rc}G_{drc}^*(\omega)\right]\\ &=1-M(\omega)\mathrm{Re}\left[k_{rc}G_{drc}^*(\omega)\right]\Big/\cos\theta(\omega)\\ &>1-M(\omega)/\max\left[M(\omega)\right]>1-1=0\end{aligned} \quad (39)$$

Thus, all the poles p_i $(i=0,1,2,\cdots)$ of the transfer function are inside the unit circle. Since k_{rc} and $M(\omega)$ are both positive, the closed-loop digital system is asymptotically stable if k_{rc} and $\theta(\omega)$ satisfy the inequalities given by Theorem 3. The proof is complete.

The relationship of k_{rc} and w_2 needs to be analyzed for further choices of the two parameters. According to [11], it is assumed that $\min|\cos\theta(\omega)|=1$ and $\max\left[M(\omega)\right]=1$ to simplify the inequality (22). Then the approximate relationship between the control gain k_{rc} and the weight w_2, can be obtained as shown in Fig. 6.

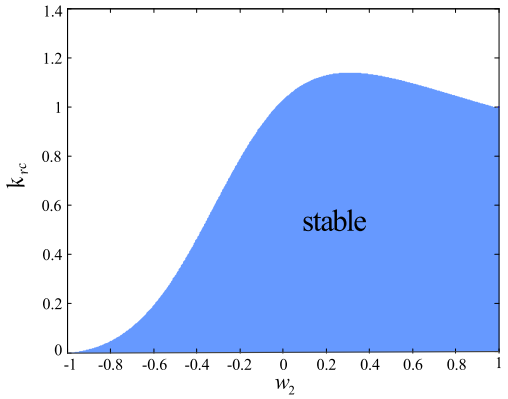

FIGURE 6. The approximately relationship between k_{rc} and w_2.

From Fig. 6, it can be found that the value of k_{rc} is greatly influenced by w_2. Specifically, when w_2 is chosen positive, there is a relatively large value range of the control gain k_{rc} to guarantee the system stability. On the contrary, when w_2 is set to be negative, the stable range of k_{rc} seems to be more restrictive with the decrease of w_2.

C. ANALYSIS OF ROBUSTNESS TO FREQUENCY FLUCTUATIONS

The frequency response of the internal model of CRC, denoted as $G_{crc}(z)$, can be expressed as:

$$|G_{crc}(\omega)|=\frac{k_{rc}}{\left|e^{j\omega T_sN}-1\right|}=\frac{1}{2}\frac{k_{rc}}{\left|\sin(\omega T_sN/2)\right|} \quad (40)$$

And the frequency response of the internal model of the novel SORC in (21) can be written as:

$$\begin{aligned}&\left|\hat{G}_{drc}(\omega)\right| \\ &= \frac{k_{rc}\left|w_1 e^{j\omega T_s N} + w_2\right|}{\left|e^{j2\omega T_s N} - w_1 e^{j\omega T_s N} - w_2\right|} \\ &= \frac{1}{2}\frac{k_{rc}}{\left|\sin(\omega T_s N/2)\right|}\sqrt{\frac{\left|1 - 4w_2 w_1 \sin^2(\omega T_s N/2)\right|}{\left|4w_2\cos^2(\omega T_s N/2) + w_1^2\right|}}\end{aligned} \tag{41}$$

where $w_1 + w_2 = 1$.

The magnitude of the novel SORC near the target frequency peak at $\omega = \omega_n = k\omega_0$, wherein $k \in \mathbb{N}$, $\omega_0 = 2\pi/T_0$, is larger than that of CRC if $-1 < w_2 < 0$, and smaller than CRC if $-1 < w_2 < 0$. This relationship can be seen by taking the magnitudes of $G_{crc}(z)$ and $\hat{G}_{drc}(z)$ for frequencies near ω_n, i.e., for $\omega = \omega_n(1+\varepsilon)$ where $|\varepsilon| \ll 1$. This yields:

$$\begin{aligned}&\frac{\left|\hat{G}_{drc}(\omega)\right|}{|G_{crc}(\omega)|} \\ &= \sqrt{\frac{\left|1 - 4w_2 w_1 \sin^2(\omega_n(1+\varepsilon)T_s N/2)\right|}{\left|4w_2\cos^2(\omega_n(1+\varepsilon)T_s N/2) + w_1^2\right|}} \\ &= \sqrt{\frac{\left|\cos^2(k\pi\varepsilon) + (2w_2-1)^2\sin^2(k\pi\varepsilon)\right|}{\left|(1+w_2)^2\cos^2(k\pi\varepsilon) + (1-w_2)^2\sin^2(k\pi\varepsilon)\right|}} \\ &= \sqrt{\frac{J_1(\varepsilon)}{J_2(\varepsilon)}}\end{aligned} \tag{42}$$

When $-1 < w_2 < 0$, thus:

$$J_1(\varepsilon) - J_2(\varepsilon) = -w_2\left[2 - w_2 - 4w_2\sin^2(k\pi\varepsilon)\right] \tag{43}$$

Due to $|\varepsilon| \ll 1$, we have $0 < \sin^2(k\pi\varepsilon) \ll 1$, so if $-1 < w_2 < 0$, the following inequity can be obtained:

$$J_1(\varepsilon) - J_2(\varepsilon) > 0 \tag{44}$$

Thus:

$$\frac{\left|\hat{G}_{drc}(\omega)\right|}{|G_{crc}(\omega)|} = \sqrt{\frac{J_1(\varepsilon)}{J_2(\varepsilon)}} > 1 \tag{45}$$

Conversely, if $0 < w_2 < 1$, we have:

$$J_1(\varepsilon) - J_2(\varepsilon) < 0 \tag{46}$$

Thus if $0 < w_2 < 1$, we have

$$\frac{\left|\hat{G}_{drc}(\omega)\right|}{|G_{crc}(\omega)|} = \sqrt{\frac{J_1(\varepsilon)}{J_2(\varepsilon)}} < 1 \tag{47}$$

This result indicates that in the vicinity of the resonant peaks at $\omega = \omega_n$, the novel SORC with $-1 < w_2 < 0$ has higher gain which is helpful in offering greater robustness to frequency fluctuations than CRC. On the contrary, if $0 < w_2 < 1$, the proposed schematic has lower gain and worse tolerance for system frequency deviation.

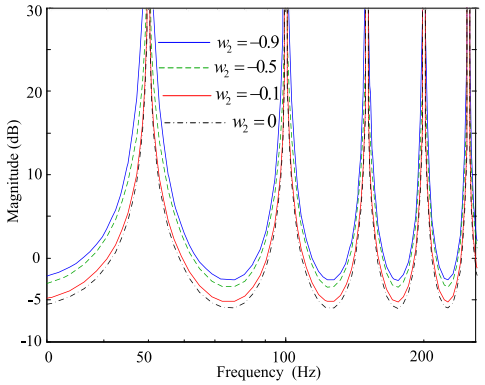

FIGURE 7. The amplitude-frequency response of $\hat{G}_{drc}(z)$ for $-1 < w_2 < 0$.

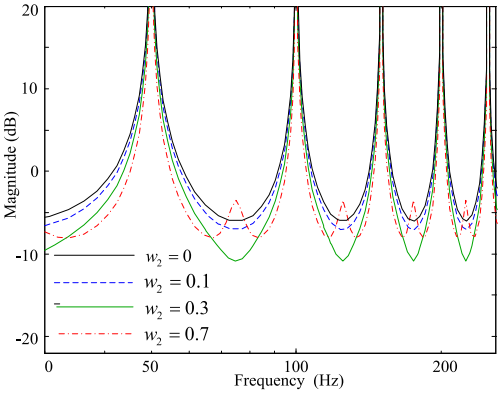

FIGURE 8. The amplitude-frequency response of $\hat{G}_{drc}(z)$ for $0 < w_2 < 1$.

Fig. 7 shows the magnitude-frequency response diagram of $\hat{G}_{drc}(z)$ for negative w_2 to examine the gain near the target frequencies. It shows that the gain near the desired harmonics becomes higher with decreasing w_2, which improves the robustness to fluctuating period. Fig. 8 shows the corresponding plot for positive w_2. As w_2 increases, the gain becomes lower than that of CRC, making the system more sensitive to period errors.

So, in order to obtain the robustness of the novel SORC, the weight w_2 should be chosen as a negative value. Moreover, Fig. 8 implies that the use of negative weight w_2 in the sensitivity transfer function can widen the notches around the fundamental frequency and its harmonics, besides, the width of notches increases as w_2 decreases.

The relationship between gain k_{rc} and weight w_2 is determined by the stability condition (22) and Fig. 6. The smaller the negative w_2 is, the better the robustness is, while the bigger value of the k_{rc}, the better dynamic performance of the system. So, the designer should make a tradeoff between robustness to period errors, and dynamic performance when tuning the set of design parameters.

IV. EXPERIMENTAL VERIFICATION

A. EXPERIMENTAL SETUP

To demonstrate the effectiveness of the proposed method, experiments are performed. Fig. 9 shows the experimental

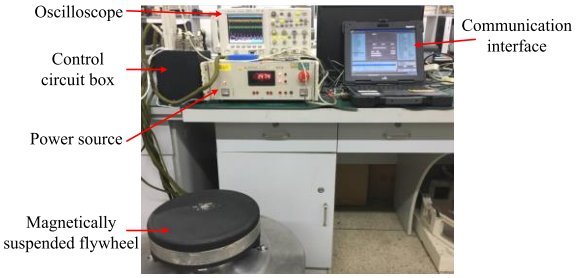

FIGURE 9. Experimental setup.

setup, with a power source, a communication interface, and a magnetically suspended flywheel prototype. The MSR system is controlled by Digital Signal Processor (DSP) TMS320C6701 and Field Programmable Gate Array (FPGA). Control updates are made at 5 kHz. The current signal and its frequency spectrum are displayed by an oscilloscope (Agilent 54624A) to illustrate the effectiveness of the current suppression.

B. THE DESIGNED PARAMETERS

The MSR system is modeled in [11] and is utilized here as a numerical example to explain the methodology of the proposed SORC design. Controllers $G_c(z)$, $G_p(z)$, and $G_w(z)$ are obtained by the Tustin transformation with a sample period T_s to discrete s-domain transfer functions that originate from attributes of the flywheel [11]:

$$\begin{aligned} G_c(s) &= \frac{0.01134s^2 + 3.4s + 4}{0.0001s^2 + s}, \\ G_w(s) &= \frac{1.4}{0.04898s + 23.1}, \\ G_p(s) &= \frac{119.26}{4.2s^2 - 372000}, \quad k_s = 36360 \end{aligned} \tag{48}$$

With these parameters, the phase range of $F(z)$ defined in (3) can be showed by the full line in Fig. 10, which is $(-90°, 270°)$.

According to (22) and (23) in Section III.B, the assurance of stability needs that the phase range of $F(z)C(z)L(z)$ should satisfy the condition of $(90°, 270°)$ and decrease the deviation from 180° as far as possible to broaden the choices of gain. Adopt the compensator design method in [11], and the compensator design result is:

$$\begin{aligned} C(z) = &\frac{1 - 0.9999z^{-1}}{1 - z^{-1}} \frac{0.084 - 0.075z^{-1}}{1 - 0.991z^{-1}} \\ &\times \left(\frac{6.556 - 6.143z^{-1}}{1 - 0.5873z^{-1}} \right)^4 \end{aligned} \tag{49}$$

$$L(z) = z^4, \quad \text{and } Q(z) = 0.25z + 0.5 + 0.25z^{-1} \tag{50}$$

and the corrected phase range is $\theta(\omega) \in (145.8°, 220.5°)$ as showed by the dotted line in Fig.10.

Based on the guidelines about the choices of w_2 in Section III.C, the different weights w_2 (0.4 and -0.4) are chosen respectively, and the robustness to the period errors of the proposed controller is tested.

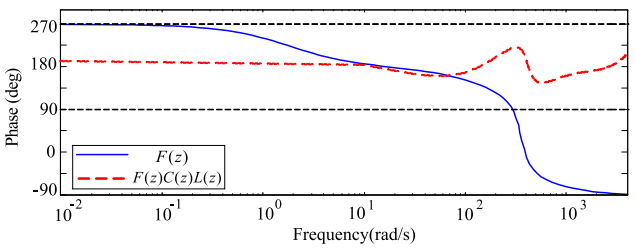

FIGURE 10. Phase-Frequency response diagram.

C. EXPERIMENTAL RESULTS AND COMPARISON

Fig. 11 shows the harmonic current in time domain and frequency domain without any harmonic suppression method. The rotation speed of the rotor is 2400 r/min, with 40Hz being the fundamental frequency.

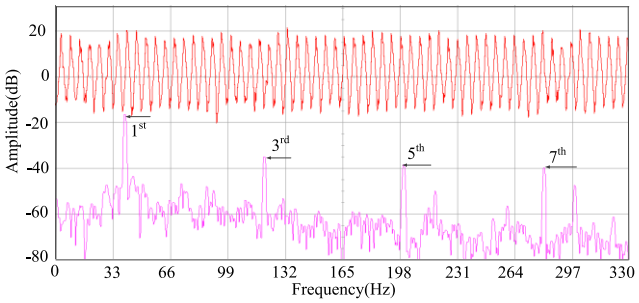

FIGURE 11. Experimental results using the closed-loop control system without repetitive control (rotation speed 2400r/min).

The upper curves in Figs. 11 and 12 are the currents in time domain. Every vertical grid represents 120 mA, and every horizontal grid represents 152ms. The lower curves show the peaks of harmonics. From Fig.11, it can be seen that there mainly exist peaks at 1st (-16.41 dB), 3rd (-34.84 dB), 5th (-38.86 dB) and 7th (-39.69 dB) orders.

In order to verify that the novel SORC has less sensitive to a period error, a frequency deviation of 0.1% is considered in Fig. 12. The results demonstrate that the novel SORC can substantially improve the performance compared with CRC.

(1) Fig. 12(a) is for CRC and still shows improvement in spite of the period deviation. The 1st peak decreases by 74.97% (from -16.41 dB to -28.44 dB), and the coil current is reduced by 80.53% (from 154.66 mA to 30.11 mA). The magnitudes of other harmonics change little. The suppression performance of CRC can't be regarded as a satisfactory result.

(2) For completeness, Fig. 12(b) is for the proposed SORC using a positive weight $w_2 = 0.4$ which is not expected to improve the robustness to period error. The 1st order harmonic is only decreased by 67.82% (from -16.41 dB to -26.26 dB), and the coil current is also reduced less by 73.7% (from 154.66 mA to 40.67 mA).

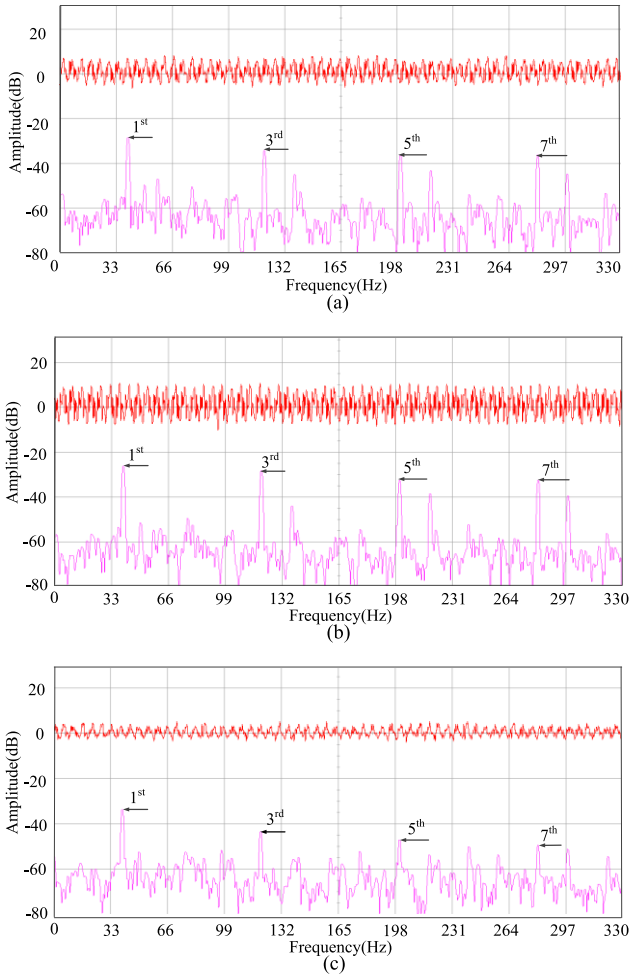

FIGURE 12. Experimental results with rotation frequency fluctuation of 0.1% (compared with 2400r/min), (a) CRC, (b) the proposed SORC with $w_2 = 0.4$, (c) the proposed SORC with $w_2 = -0.4$.

The result is worse than that of CRC. The choice of positive weight w_2 indeed gives rise to a reduction in the robustness to fluctuations, which is in consistent with previous prove.

(3) Fig. 12(c) uses $w_2 = -0.4$ and the expected substantial improvement is observed. The magnitudes of harmonics at the 1st, 3rd, 5th and 7th orders are decreased by 86.38% (from −16.41 dB to −33.73 dB), 62.67% (−34.84 dB to −43.4 dB), 60.96% (from −38.86 dB to −47.03 dB), and 67.23% (from −39.69 dB to −49.38 dB), respectively. The value of coil current is reduced by 90.06% (from 154.66 mA to 15.37 mA). The controller under errors still works well.

The comparison in Fig.12 shows that the SORC can introduce a better capacity of resisting frequency fluctuations into the MSR system, which is an urgent need in micro-vibration spacecrafts.

V. CONCLUSION

Higher order repetitive control is developed as a method of making repetitive control less sensitive to accurate knowledge of the disturbance period, or less sensitive to fluctuations of the period in hardware implementation. Stability conditions for such systems are impractical to use, so that people develop various sufficient conditions. However, the sufficient stability conditions which are easy to use are very conservative, making people have trouble in designing effective higher order repetitive control and ensuring the stability. Motivated by application of repetitive control to suppress vibrations from magnetically suspended rotors in spacecraft attitude control actuators, a novel second order repetitive control is developed. In spite of the name second order, it does not need data from two periods in the past. This allows us to create a stability condition that is much less conservative and much more useful in the design of second order repetitive control. Hardware experiments demonstrate the effectiveness of the novel stability criterion in the design of second order repetitive control.

REFERENCES

[1] J. Fang and Y. Ren, "High-precision control for a single-gimbal magnetically suspended control moment gyro based on inverse system method," *IEEE Trans. Ind. Electron.*, vol. 58, no. 9, pp. 4331–4342, Sep. 2011.

[2] S. G. Edwards, B. N. Agrawal, and M. Q. Phan, "Disturbance identification and rejection experiments on an Ultra Quiet Platform," *Adv. Astronaut. Sci.*, vol. 103, pp. 633–651, 2000.

[3] E. S. Ahn, R. W. Longman, B. N. Agrawal, and J. J. Kim, "Evaluation of five control algorithms for addressing CMG induced jitter on a spacecraft testbed," *J. Astronaut. Sci.*, vol. 60, nos. 3–4, pp. 434–467, 2013.

[4] S. Sivrioglu and K. Nonami, "Sliding mode control with time-varying hyperplane for AMB systems," *IEEE/ASME Trans. Mechatronics*, vol. 3, no. 1, pp. 51–59, Mar. 1998.

[5] M. S. Kandil, M. R. Dubois, J. P. F. Trovão, and L. S. Bakay, "Application of second-order sliding-mode concepts to active magnetic bearings," *IEEE Trans. Ind. Electron*, vol. 65, no. 1, pp. 855–864, Jan. 2018.

[6] C. Peng, J. Sun, X. Song, and J. Fang, "Frequency-varying current harmonics for active magnetic bearing via multiple resonant controllers," *IEEE Trans. Ind. Electron.*, vol. 64, no. 1, pp. 517–526, Jan. 2017.

[7] J. Yao, Z. Jiao, and D. Ma, "A practical nonlinear adaptive control of hydraulic servomechanisms with periodic-like disturbances," *IEEE/ASME Trans. Mechatronics*, vol. 20, no. 6, pp. 2752–2760, Dec. 2015.

[8] S. Zheng, Q. Chen, and H. Ren, "Active balancing control of AMB-rotor systems using a phase-shift notch filter connected in parallel mode," *IEEE Trans. Ind. Electron.*, vol. 63, no. 6, pp. 3777–3785, Jun. 2016.

[9] P. Cui, S. Li, C. Peng, and G. Zhao, "Suppression of harmonic current in active–passive magnetically suspended CMG using improved repetitive controller," *IEEE/ASME Trans. Mechatronics*, vol. 21, no. 4, pp. 2132–2141, Aug. 2016.

[10] S. Yang, P. Wang, Y. Tang, M. Zagrodnik, X. Hu, and K. J. Tseng, "Circulating current suppression in modular multilevel converters with even-harmonic repetitive control," *IEEE Trans. Ind. Appl.*, vol. 54, no. 1, pp. 298–309, Jan. 2018.

[11] P. Cui, Q. Wang, Q. Gao, and G. Zhang, "Hybrid fractional repetitive control for magnetically suspended rotor systems," *IEEE Trans. Ind. Electron.*, vol. 65, no. 4, pp. 3491–3498, Apr. 2018.

[12] M. Steinbuch, "Repetitive control for systems with uncertain period-time," *Automatica*, vol. 38, no. 12, pp. 2103–2109, Dec. 2002.

[13] C.-P. Lo and R. W. Longman, "Root locus analysis of higher order repetitive control," *Adv. Astronaut. Sci.*, vol. 120, pp. 2021–2040, 2005.

[14] C.-P. Lo and R. W. Longman, "Frequency response analysis of higher order repetitive control," *Adv. Astronaut. Sci.*, vol. 123, pp. 1183–1202, 2006.

[15] M. Steinbuch, S. Weiland, and T. Singh, "Design of noise and period-time robust high-order repetitive control, with application to optical storage," *Automatica*, vol. 43, no. 12, pp. 2086–2095, Dec. 2007.

[16] G. Pipeleers, B. Demeulenaere, J. De Schutter, and J. Swevers, "Robust high-order repetitive control: Optimal performance trade-offs," *Automatica*, vol. 44, no. 10, pp. 2628–2634, Oct. 2008.

[17] G. A. Ramos and R. Costa-Castelló, "Power factor correction and harmonic compensation using second-order odd-harmonic repetitive control," *IET Control Theory Appl.*, vol. 6, no. 11, pp. 1633–1644, Jul. 2012.
[18] G. A. Ramos, R. Costa-Castelló, J. M. Olm, and R. Cardoner, "Robust high-order repetitive control of an active filter using an odd-harmonic internal model," in *Proc. IEEE Int. Symp. Ind. Electron.*, Jul. 2010, pp. 1040–1045.
[19] R. Costa-Castelló, J. M. Olm, M. Steinbuch, and G. A. Ramos, "Second-order odd-harmonic repetitive control and its application to active filter control," in *Proc. 49th IEEE Conf. Decis. Control (CDC)*, Atlanta, GA, USA, vol. 58, Dec. 2010, pp. 6967–6972.
[20] H. J. Guo, R. W. Longman, and T. Ishihara, "A design approach for insensitivity to disturbance period fluctuations using higher order repetitive control," in *Proc. 19th World Congr. Int. Fed. Autom. Control*, Cape Town, South Africa, 2014, pp. 6508–6513.
[21] E. S. Ahn, R. W. Longman, and J. J. Kim, "Comparison of multiple-period and higher order repetitive control used to produce robustness to period fluctions," *Adv. Astronaut. Sci.*, vol. 148, pp. 179–202, 2013.
[22] Y. Wang and R. W. Longman, "Monotonic vibration suppression using repetitive control and windowing techniques," *Adv. Astronaut. Sci.*, vol. 93, pp. 945–965, 1996.
[23] R. W. Longman and S.-L. Wirkander, "Automated tuning concepts for iterative learning and repetitive control laws," in *Proc. 37th IEEE Conf. Decis. Control*, Tampa, FL, USA, Dec. 1998, pp. 192–198.
[24] Y. Wang, D. Wang, B. Zhang, Y. Ye, and K. Zhou, "Robust repetitive control with linear phase lead," in *Proc. Amer. Control Conf.*, Minneapolis, MN, USA, Jun. 2016, pp. 232–237.
[25] R. W. Longman, "Iterative learning control and repetitive control for engineering practice," *Int. J. Control*, vol. 73, no. 10, pp. 930–954, 2000.
[26] R. W. Longman, "On the theory and design of linear repetitive control systems," *Eur. J. Control*, vol. 16, no. 5, pp. 447–496, 2010.
[27] S. Songschon and R. W. Longman, "Comparison of the stability boundary and the frequency response stability condition in learning and repetitive control," *Int. J. Appl. Math. Comput. Sci.*, vol. 13, no. 2, pp. 169–177, 2003.

PEILING CUI (M'12) was born in Henan, China, in 1975. She received the Ph.D. degree in control theory and control engineering from Northwestern Polytechnical University, Xi'an, China, in 2004. She is currently an Associate Professor with the School of Instrumentation and Optoelectronic Engineering, Beihang University, Beijing, China. Her current research interest includes the active vibration control of magnetically suspended rotor.

ZHIYUAN LIU received the B.S. degree in automation from Northwestern Polytechnical University, Xi'an, China, in 2017. He is currently pursuing the M.S. degree with Beihang University, Beijing, China. His current research interest includes the active vibration control of magnetically suspended control moment gyro.

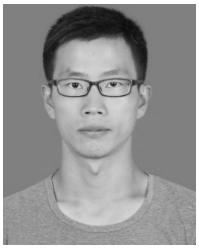

GUOXI ZHANG received the B.S. degree in measurement and control technology and instrumentation from Northwestern Polytechnical University, Xi'an, China, in 2016. He is currently pursuing the M.S. degree with Beihang University, Beijing, China. His current research interest includes the active vibration control of magnetically suspended control moment gyro.

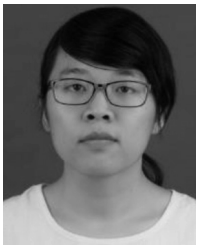

HAN XU received the B.S. degree in automation from Shandong University, Jinan, China, in 2017. She is currently pursuing the M.S. degree with Beihang University, Beijing, China. Her current research interest includes the active vibration control of magnetically suspended control moment gyro.

RICHARD W. LONGMAN received the Ph.D. degree in aerospace engineering from the University of California at San Diego, San Diego, in 1969. He held the Distinguished Romberg Guest Professorship with Heidelberg University, Germany. Since 1970, he has been a Professor of mechanical engineering and civil engineering & engineering mechanics with Columbia University. His current research interests include iterative learning control, repetitive control, stable inverses, and system identification, especially the active vibration control of magnetically suspended rotor. He served for the American Astronautical Society, as a Vice President of Publications, VP-Technical, First VP, and a Member of the Board of Directors. He was a recipient of the Alexander von Humboldt Award for lifetime achievement in research.